

**Long Range Charge Transfer in Trimetallic Mixed-Valence Iron Complexes
Mediated by Redox Non-Innocent Cyanoacetylide Ligands**

*Josef B. G. Gluyas, Andrew J. Boden, Samantha G. Eaves, Herrick Yu and Paul. J.
Low**

*Dr. Josef B. G. Gluyas, Andrew J. Boden, Samantha G. Eaves, Herrick Yu
Durham University, Department of Chemistry
Science Site, South Road, Durham, DH1 3LE, UK*

*W/Prof. Paul J. Low
Durham University, Department of Chemistry
Science Site, South Road, Durham, DH1 3LE, UK
School of Chemistry and Biochemistry, University of Western Australia
Crawley, Perth, 6009, Australia.
E-mail: paul.low@uwa.edu.au*

Contents

General Conditions	2
Synthetic Details	3
UV-vis-NIR and IR Spectroelectrochemistry	6
Gaussian Deconvolutions	9
Visible Spectra of [4][BF₄]₂ and [5][BF₄]₂	10
Crystal Structure Analysis of [3][BF₄]₂	10
Estimation of the Length of [4][BF₄]₂ and [5][BF₄]₂	13
Cyclic Voltammetry	13
References	15

General Conditions

All reactions were carried out under an atmosphere of dry nitrogen using standard Schlenk techniques. Acetonitrile, dichloromethane and toluene were purified and dried using an Innovative Technology SPS-400 before use, all other solvents were standard reagent grade and used as received. No special precautions were taken to exclude air or moisture during workup except where otherwise indicated. The compounds $[\text{Fe}(=\text{C}=\text{CH}_2)(\text{dppe})\text{Cp}][\text{PF}_6]$,^{S1} 1-cyano-4-dimethyl-amino pyridinium tetrafluoroborate ($[\text{CAP}]\text{BF}_4$),^{S2} and $[\text{Fe}(\text{dppe})_2(\text{MeCN})_2][\text{BF}_4]_2$ ($[\mathbf{2}][\text{BF}_4]_2$)^{S3} were prepared by literature routes. All other reagents were commercially available and used as received. Column chromatography was performed using silica gel. NMR spectra were recorded at 23 °C on a Varian NMR Systems 700 (¹H, 699.7 MHz; ¹³C, 175.9 MHz; ³¹P, 283.3 MHz) or a Bruker Avance III HD 400 (¹H, 400.1 MHz; ³¹P, 162.0 MHz) spectrometer using CDCl_3 , CD_2Cl_2 or CD_3CN as the solvent. Chemical shifts were determined relative to internal CHCl_3 (¹H, $\delta = 7.26$ ppm; CDCl_3), CH_2Cl_2 (¹H, $\delta = 5.32$ ppm; CD_2Cl_2), internal CD_2HCN (¹H, $\delta = 1.94$ ppm; CD_3CN), internal CD_2Cl_2 (¹³C, $\delta = 53.8$ ppm; CD_2Cl_2)^{S4} or external H_3PO_4 (85%, ³¹P, $\delta = 0.00$ ppm; CDCl_3 , CD_2Cl_2 , CD_3CN). Positive mode ESI mass spectrometry was carried out using a Waters Micromas LCT Spectrometer from solutions in methanol or acetonitrile. IR spectra were recorded on a Nicolet Avatar 6700 FT-IR from samples in Nujol mounted between NaCl discs or using solution cells fitted with CaF_2 windows. Elemental analyses were performed at the London Metropolitan University.

Cyclic voltammetry was carried out using an EcoChemie Autolab PG-STAT 30 or a Palm Instruments EmStat3⁺ potentiostat, with a platinum disc working electrode, a platinum wire counter electrode, and a platinum wire pseudo-reference electrode, from solutions in acetonitrile and dichloromethane containing either 0.1 M NBu_4PF_6 or 0.1 M $\text{NBu}_4[\text{B}\{\text{C}_6\text{H}_3(\text{CF}_3)_{2-3,5}\}_4]$ as the electrolyte. Measurements with $v = 100, 200, 400$ and $800 \text{ mV}\cdot\text{s}^{-1}$ showed that the ratio of the anodic to cathodic peak currents varied linearly as a function of the square root of scan rate in all cases. The decamethylferrocene/decamethylferrocinium ($\text{FeCp}^*_2/[\text{FeCp}^*_2]^+$) couple was used as an internal reference for potential measurements such that the couple falls at -0.55 V ($\text{CH}_2\text{Cl}_2 / \text{NBu}_4\text{PF}_6$), -0.62 V ($\text{CH}_2\text{Cl}_2 / \text{NBu}_4\text{BAr}^{\text{F}_4}$) or -0.51 V ($\text{MeCN} / \text{NBu}_4\text{PF}_6$) relative to external $\text{FeCp}_2/[\text{FeCp}_2]^+$ at 0.00 V as determined by in-house calibration.

Spectroelectrochemical measurements were made in an OTTLE cell of Hartl design,^{S5} from acetonitrile or dichloromethane containing 0.1 M NBu₄PF₆ as the electrolyte. The cell was fitted into the sample compartment of a Nicolet Avatar 6700 FT-IR or an Agilent Technologies Cary 5000 UV-vis-NIR spectrophotometer, and electrolysis in the cell was performed with a Palm Instruments EmStat² potentiostat.

Synthetic Details

Fe(C≡CC≡N)(dppe)Cp (1).

The compound [Fe(=C=CH₂)(dppe)Cp]PF₆ (510 mg, 739 μmol) and potassium *tert*-butoxide (150 mg, 1.34 mmol) were added to dry degassed CH₂Cl₂ (15 mL) and stirred for thirty minutes, yielding a deep orange solution. A sample of 1-cyano-4-dimethyl-amino pyridinium tetrafluoroborate ([CAP]BF₄) (210 mg, 894 μmol) was then added and the reaction was stirred for a further twenty minutes, yielding a deep red solution. The reaction mixture was filtered and filtrate concentrated to dryness leaving a dark oily red residue, which was purified by column chromatography (eluent 70:30, hexanes/acetone (v/v)) A yellow / orange band was collected and solvent removed under reduced pressure to afford **1** as an orange solid in 71% yield (300 mg, 527 μmol). ¹H NMR (400.1 MHz, CDCl₃): δ = 2.13–2.32 (m, 2H, dppe), 2.48 – 2.59 (m, 2H, dppe), 4.22 (s, 5H, C₅H₅), 7.28–7.69 (m, 20H, dppe). ³¹P NMR (162.0 MHz, CD₂Cl₂): δ = 102.9. IR (CH₂Cl₂): ν(C≡CC≡N) 1991, 2174 cm⁻¹. ESI-MS: m/z(%) 569 (100) [M]⁺.

[Fe(dppm)₂(MeCN)₂][BF₄]₂ ([3][BF₄]₂).

A solution of diphenylphosphinomethane (934 mg, 2.43 mmol) in toluene (4 ml) was added to a solution of [Fe(H₂O)₆][BF₄]₂ (400 mg, 1.19 mmol) in acetonitrile (2 ml) and the resulting mixture was heated at reflux for 14 h and then allowed to cool to ambient temperature. Cooling resulted in crystallization. The resulting solid was isolated by filtration and dried under vacuum to afford ([3][BF₄]₂) in 43% yield as bright red crystals (553 mg, 512 μmol). ¹H NMR (400.1 MHz, CD₃CN): δ = 1.45 (s, 6 H, CH₃CN), 5.17 (s, 4 H, dppm), 7.09 (m, 16 H, dppm), 7.38–7.59 (m, 24 H, dppm) ppm. ³¹P NMR (162.0 MHz, CD₃CN): δ = 11.5 ppm. IR (Nujol): ν(C≡N) 2268 cm⁻¹. ESI-MS: m/z(%) 413 (100) [M – 2BF₄ – 2MeCN]²⁺.

[trans-Fe{N≡CC≡CFe(dppe)Cp}₂(dppe)₂][BF₄]₂ ([4][BF₄]₂)

Compound **1** (50.0 mg, 81.3 μmol) was added to a solution of **[2][BF₄]₂** (97.0 mg, 89.8 μmol) in acetonitrile (1 ml). The resulting solution was heated to reflux for 3 h and then allowed to cool to ambient temperature. The precipitate that had formed was recovered by filtration and washed with cold (0 °C) diethylether (2 × 10 ml) to afford **[4][BF₄]₂** in 95% yield (relative to **1**) as a khaki green solid (84.0 mg, 38.8 μmol). ¹H NMR (699.7 MHz, CD₂Cl₂): δ = 2.50 (m, 12 H, dppe), 2.62 (m, 4 H, dppe), 4.42 (s, 10 H, C₅H₅), 6.68 (m, 16 H, *o*-C₆H₅, Fe(dppe)₂), 6.90 (m, 16 H, *m*-C₆H₅, Fe(dppe)₂), 7.05 (m, 8 H, *o*-C₆H₅, Fe(dppe)Cp), 7.23 (m, 8 H, *m*-C₆H₅, Fe(dppe)Cp), 7.31 (m, 8 H, *m*-C₆H₅, Fe(dppe)Cp), 7.37 (m, 16 H, *p*-C₆H₅, Fe(dppe)₂), 7.42 (m, 8 H, *p*-C₆H₅, Fe(dppe)Cp), 7.59 (m, 8 H, *o*-C₆H₅, Fe(dppe)Cp) ppm. ¹³C NMR (175.9 MHz, CD₂Cl₂): δ = 28.8–29.3 (m, Ph₂PCH₂CH₂PPh₂), 82.5 (s, C₅H₅), 128.8 (m, *m*-C₆H₅, Fe(dppe)Cp), 129.0–129.1 (m, *m*-C₆H₅, Fe(dppe)Cp and Fe(dppe)₂), 130.4 (m, *o*-C₆H₅, Fe(dppe)Cp), 131.1 (m, *o*-C₆H₅, Fe(dppe)Cp), 131.2 (m, *o*-C₆H₅, Fe(dppe)₂), 131.5–131.7 (m, *i*-C₆H₅), 131.7 (m, *p*-C₆H₅, Fe(dppe)Cp), 133.4 (m, *p*-C₆H₅, Fe(dppe)₂), 133.7 (m, *p*-C₆H₅, Fe(dppe)Cp), 135.7–136.0 (m, *i*-C₆H₅), 139.3–139.5 (m, *i*-C₆H₅) ppm, C≡CC≡N not observed. ³¹P NMR (283.3 MHz, CD₂Cl₂): δ = 51.4 (Fe(dppe)₂), 102.3 (Fe(dppe)Cp) ppm. IR (CH₂Cl₂): ν(C≡CC≡N) 1957, 2178 cm⁻¹. ESI-MS: m/z(%) 995 (100) [M – 2BF₄]²⁺. Found: C, 66.38; H, 4.85; N, 1.39. Calc. for C₁₂₀H₁₀₆B₂N₂F₈P₈Fe₃: C, 66.57; H, 4.93; N, 1.29%

[trans-Fe{N≡CC≡CFe(dppe)Cp}₂(dppm)₂][BF₄]₂ ([5][BF₄]₂)

Compound **1** (96.0 mg, 162 μmol) was added to a solution of **[3][BF₄]₂** (100 mg, 93.0 μmol) in acetonitrile (1 ml). The resulting solution was heated to reflux for 3 h and then allowed to cool to ambient temperature. The precipitate that had formed was recovered by filtration and washed with cold (0 °C) diethylether (2 × 10 ml) to afford **[5][BF₄]₂** in 62% yield (relative to **1**) as a brick red solid (108 mg, 50.5 μmol). ¹H NMR (699.7 MHz, CD₂Cl₂): δ = 2.43 (m, 8 H, dppe), 4.29 (s, 10 H, C₅H₅), 5.10 (m, 4H, dppm), 6.82 (m, 16 H, *o*-C₆H₅, Fe(dppm)₂), 6.94 (m, 16 H, *m*-C₆H₅, Fe(dppm)₂), 6.99 (m, 8 H, *o*-C₆H₅, Fe(dppe)Cp), 7.23 (m, 8 H, *m*-C₆H₅, Fe(dppe)Cp), 7.28 (m, 8 H, *m*-C₆H₅, Fe(dppe)Cp), 7.33 (m, 8 H, *o*-C₆H₅, Fe(dppe)Cp), 7.41 (m, 8 H, *p*-C₆H₅, Fe(dppe)Cp), 7.46 (m, 12 H, *p*-C₆H₅, Fe(dppe)Cp and *p*-C₆H₅,

Fe(dppm)₂) ppm. ¹³C NMR (175.9 MHz, CD₂Cl₂): δ = 27.9–28.1 (m, Ph₂PCH₂CH₂PPh₂), 47.8 (m, Ph₂PCH₂PPh₂), 82.2 (s, C₅H₅), 128.7–128.8 (m, *m*-C₆H₅, Fe(dppe)Cp), 129.6 (m, *m*-C₆H₅, Fe(dppm)₂), 130.5 (m, *o*-C₆H₅, Fe(dppe)Cp), 130.7–130.8 (m, *i*-C₆H₅), 131.1 (m, *o*-C₆H₅, Fe(dppe)Cp), 131.4 (m, *o*-C₆H₅, Fe(dppm)₂), 132.2 (m, *o*-C₆H₅, Fe(dppe)Cp), 133.2 (m, *o*-C₆H₅, Fe(dppm)₂ and Fe(dppe)Cp), 137.1–137.4 (m, *i*-C₆H₅), 138.7–138.9 (m, *i*-C₆H₅) ppm, C≡CC≡N not observed. ³¹P NMR (283.3 MHz, CD₂Cl₂): δ = 8.2 (Fe(dppm)₂), 102.6 (Fe(dppe)Cp) ppm. IR (CH₂Cl₂): ν(C≡CC≡N) 1964, 2180 cm⁻¹. ESI-MS: m/z(%) 981 (100) [M – 2BF₄]²⁺. Found: C, 66.25; H, 4.92; N, 1.36. Calc. for C₁₁₈H₁₀₂B₂N₂F₈P₈Fe₃: C, 66.32; H, 4.81; N, 1.31%

Spectroelectrochemistry

Spectroelectrochemical investigation of both compounds $[4][BF_4]_2$ and $[5][BF_4]_2$ were carried out in dichloromethane / 0.1 M NBu_4PF_6 , and also in NCMe / 0.1 M NBu_4PF_6 in the case of $[4][BF_4]_2$. The poor solubility of both complexes in other solvent systems compatible with spectroelectrochemical experiments, along with the instability of $[5][BF_4]_2$ in acetonitrile prevented further solvatochromic investigations.

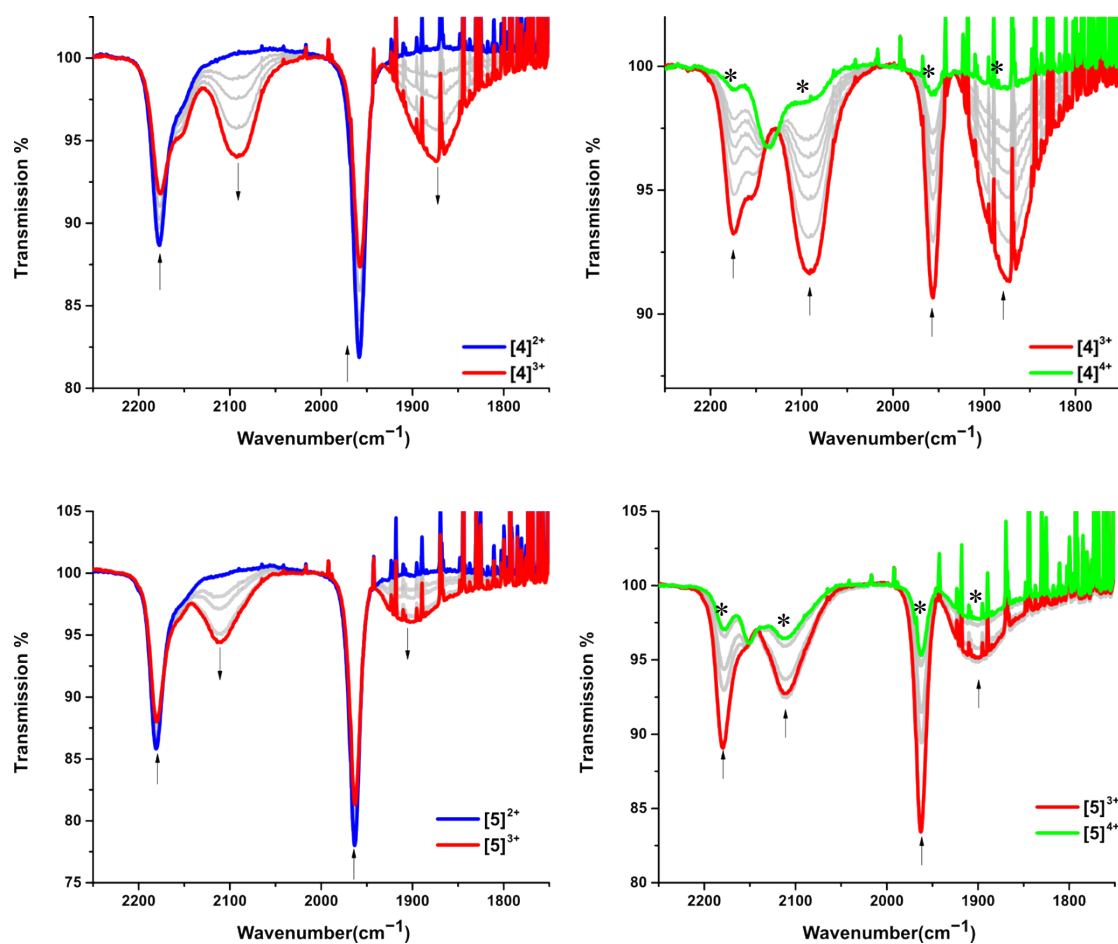


Figure S1. IR spectra of $[4][BF_4]_2$ (upper) and $[5][BF_4]_2$ (lower) obtained spectroelectrochemically in dichloromethane utilising 0.1 M NBu_4PF_6 as the supporting electrolyte. * Residual bands of the trications.

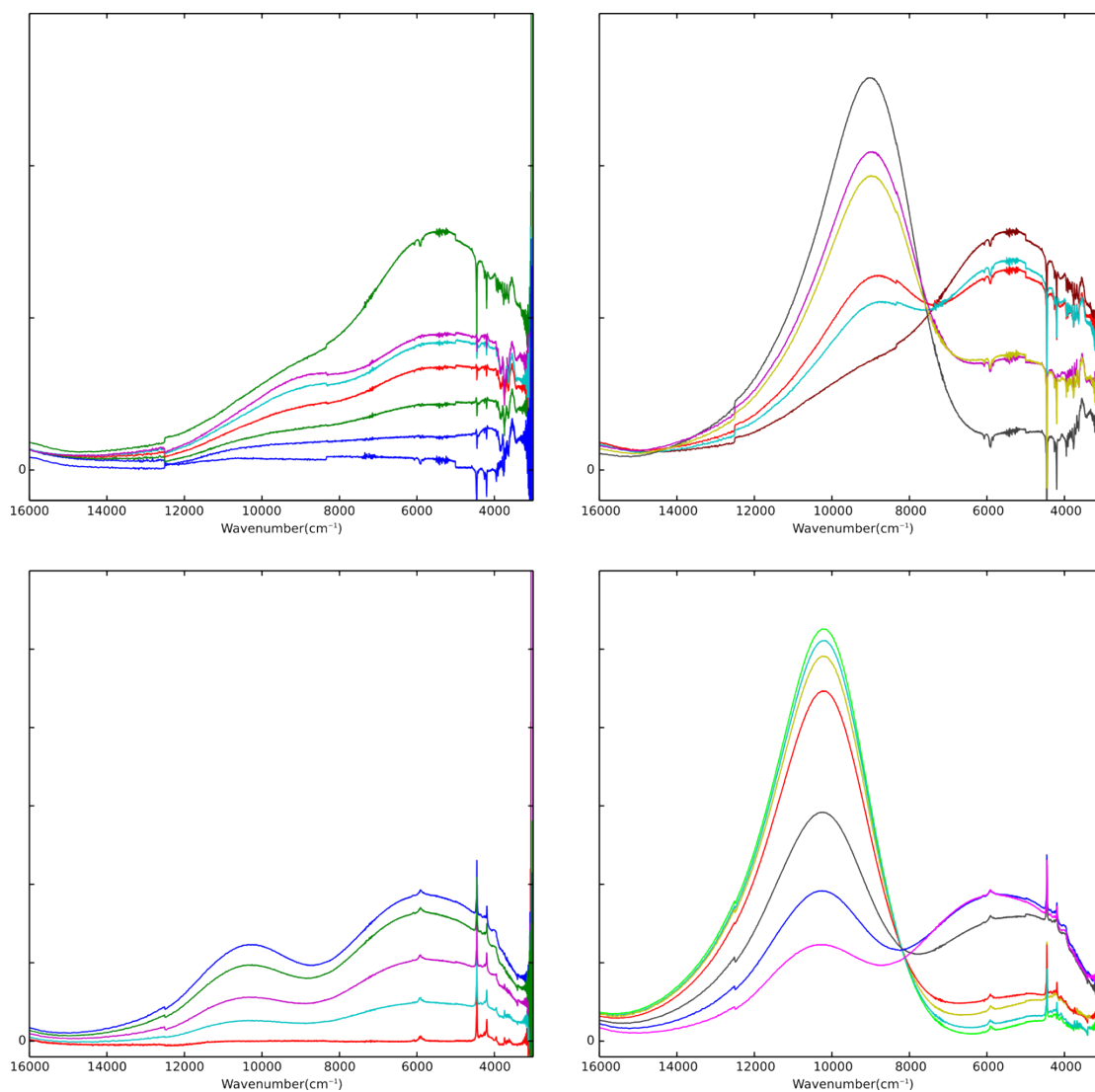


Figure S2. UV-Vis-NIR spectra of $[4]^{n+}$ ($n = 2 \rightarrow 3$ upper left, $n = 3 \rightarrow 4$ upper right) and $[5]^{n+}$ ($2 \rightarrow 3$ lower left, $n = 3 \rightarrow 4$ lower right) obtained spectroelectrochemically in dichloromethane utilising NBu_4PF_6 as the supporting electrolyte plotted against an arbitrary absorbance scale.

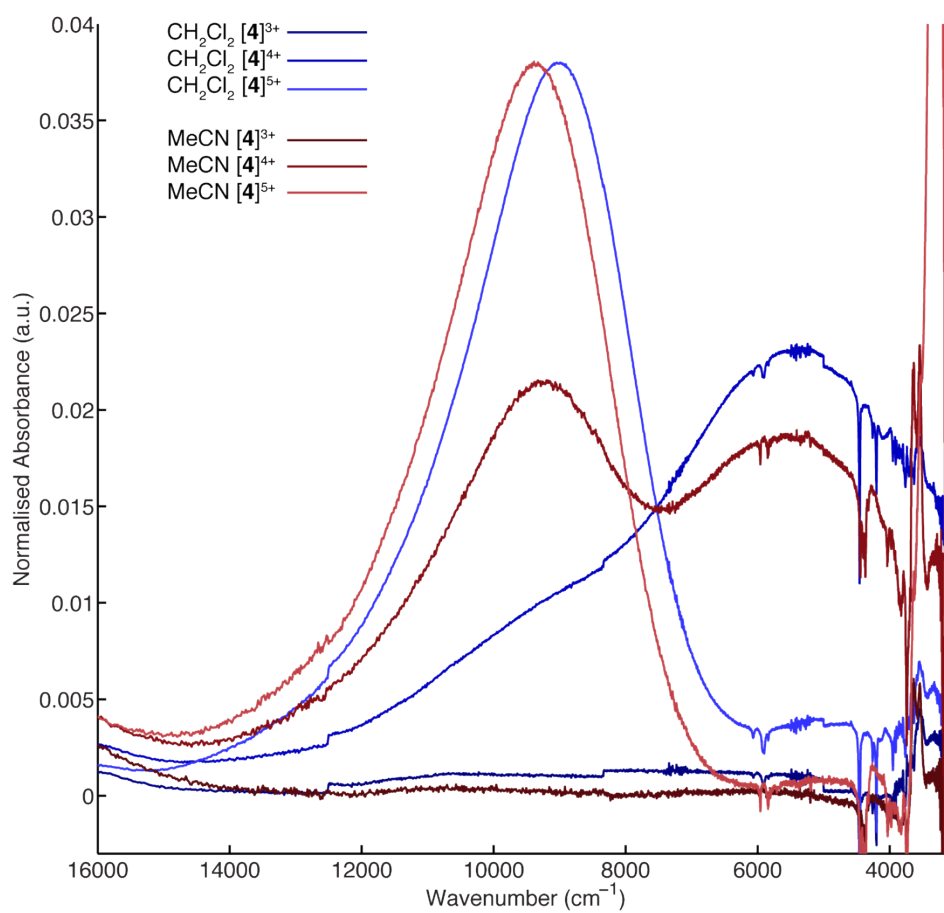


Figure S3. Overlapping UV-Vis-NIR spectra of [4]ⁿ⁺ obtained spectroelectrochemically in acetonitrile (red) and dichloromethane (blue) utilising NBU₄PF₆ as the supporting electrolyte illustrating the solvatochromic behavior.

Gaussian Deconvolutions

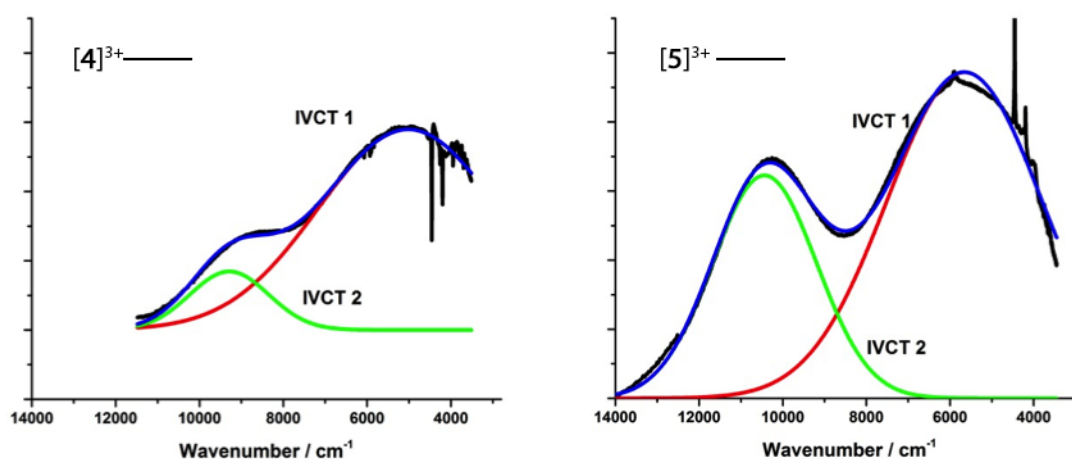


Figure S4. Deconvoluted UV-Vis-NIR spectra of $[4]^{3+}$ (left) and $[5]^{3+}$ (right) obtained spectroelectrochemically in dichloromethane utilising NBu_4PF_6 as the supporting electrolyte. The red and green lines show the separate IVCT events as obtained by Gaussian deconvolution and the blue line represents the sum of the fitted curves plotted against an arbitrary absorbance scale.

		$[4]^{3+}$	$[5]^{3+}$
IVCT 1	$1/\lambda$ (cm^{-1})	5018	5655
	FWHM (cm^{-1})	5062	4365
	ϵ ($\text{mol}^{-1} \text{cm}^{-1}$)	5796	9438
	H_{ab} (Class II) (cm^{-1})	610	665
	$\nu_{1/2}$ (Hush)	3404	3616
IVCT 2	$1/\lambda$ (cm^{-1})	9290	10435
	FWHM (cm^{-1})	2212	2938
	ϵ ($\text{mol}^{-1} \text{cm}^{-1}$)	1690	6453
	H_{ab} (Class III) (cm^{-1})	1845	1469
	$\nu_{1/2}$ (Hush)	4632	4910

Table S1. Experimental parameters from the deconvoluted bands of the UV-Vis-NIR of $[4]^{3+}$ and $[5]^{3+}$.

Visible Absorption Spectra

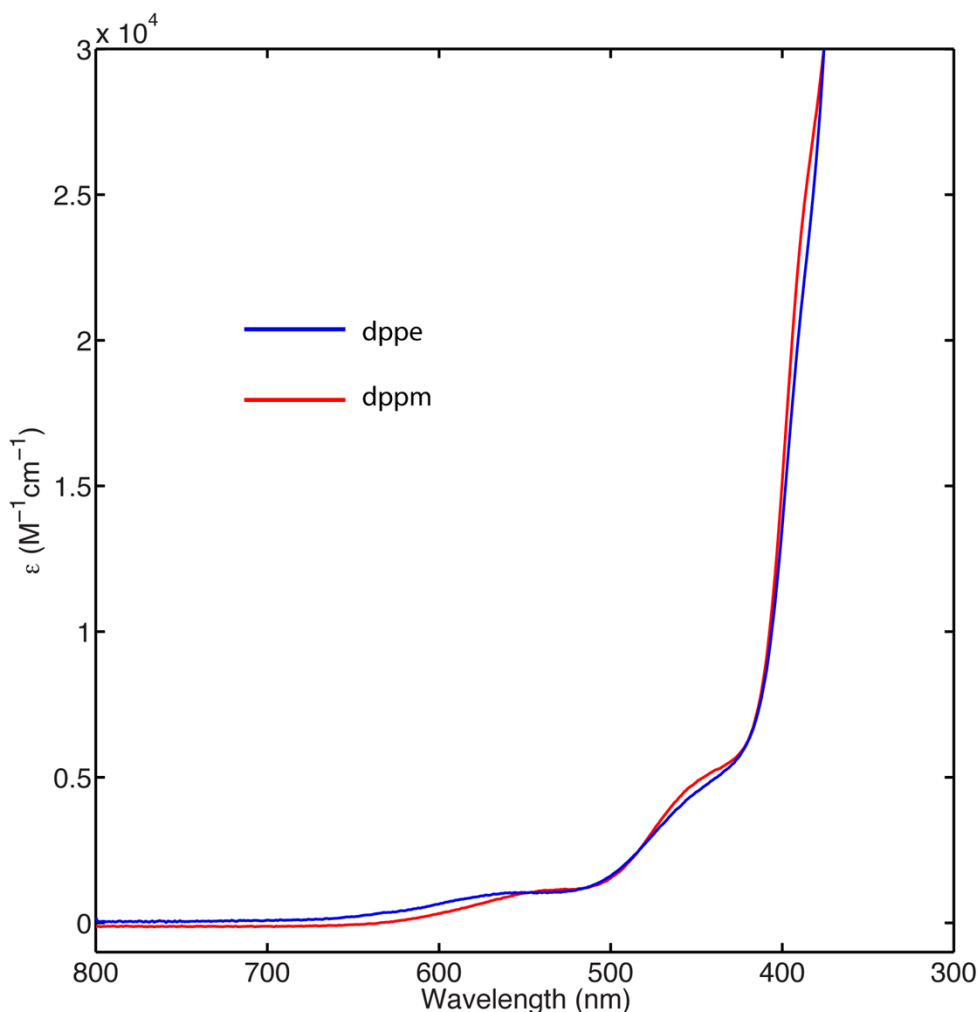


Figure S5. Comparison of the visible absorption spectra of $[4][BF_4]_2$ (blue) and $[5][BF_4]_2$ (red).

Crystal Structure Analysis

A suitable single crystal of $[3][BF_4]_2$ was obtained directly following the procedure described in the experimental section. The X-ray single crystal data for $[3][BF_4]_2$ were collected at 120.0(2) K on a Bruker D8 Venture diffractometer ($I\mu S$ microsource, focusing mirrors, $\lambda MoK\alpha$, $\lambda = 0.71073 \text{ \AA}$) equipped with a Cryostream (Oxford Cryosystems) open-flow nitrogen cryostat. The structures was solved by direct

method and refined by full-matrix least squares on F^2 for all data using Olex2^{S6} and SHELXTL^{S7} software. All non-hydrogen atoms were refined anisotropically, hydrogen atoms were placed in the calculated positions and refined in riding mode. Crystal data and parameters of refinement are listed in Table S2. Crystallographic data for the structure have been deposited with the Cambridge Crystallographic Data Centre as supplementary publication CCDC-973687.

The structure contains two independent cations of slightly different conformation both located in the centres of symmetry, two tetrafluoroborate anions and two acetonitrile molecules. The anions and solvent molecules are arranged so as to fill the gaps between columns of cations.

Empirical formula	$C_{54}H_{50}FeN_4P_4 \times 2 BF_4 \times 2 CH_3CN$
Formula weight	1162.42
Temperature/K	120
Crystal system	Monoclinic
Space group	$P2_1/n$
a/Å	16.8867(6)
b/Å	15.6956(6)
c/Å	21.8725(8)
$\alpha/^\circ$	90.00
$\beta/^\circ$	106.957(2)
$\gamma/^\circ$	90.00
Volume/Å ³	5545.2(4)
Z	4
$\rho_{calc}/mg/mm^3$	1.392
m/mm^{-1}	0.457
F(000)	2400.0
Crystal size/mm ³	$0.291 \times 0.239 \times 0.165$
2 Θ range for data collection	3.74 to 60°
Index ranges	$-23 \leq h \leq 20, -22 \leq k \leq 22, -20 \leq l \leq 30$
Reflections collected	83155
Independent reflections	16176[R(int) = 0.0496]
Data/restraints/parameters	16176/0/701
Goodness-of-fit on F ²	0.998
Final R indexes [$I \geq 2\sigma(I)$]	$R_1 = 0.0390, wR_2 = 0.0928$
Final R indexes [all data]	$R_1 = 0.0606, wR_2 = 0.1034$
Largest diff. peak/hole / e Å ⁻³	0.67/-0.45

Table S2. Crystal data and structure refinement for **[3]**[BF₄]₂

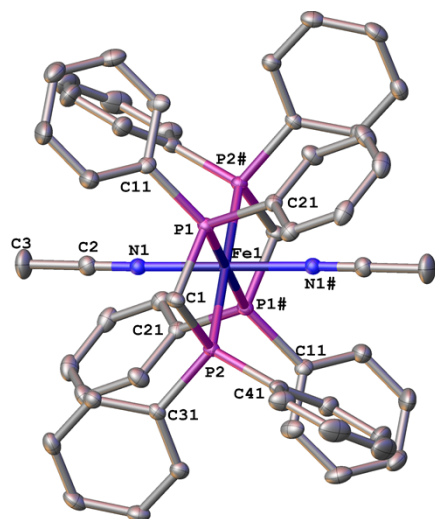


Figure S6. The molecular structure of the cation of $[3]^{2+}$ in the crystal of $[3][BF_4]_2$. Selected bond lengths [\AA] and angles [deg]: N1–Fe1 1.897(1), P1–Fe1 2.2884(3), P2–Fe1 2.2960(4); N1–Fe1–N1# 180.00(6), P1–Fe1–P1# 180.00(1), P2–Fe1–P2# 180.00(1), P1–C1–P2 95.51(8), P1–Fe1–P2 72.64(1).

Estimation of the Length of $[4][BF_4]_2$ and $[5][BF_4]_2$

The distance between the peripheral iron centres in $[4][BF_4]_2$ and $[5][BF_4]_2$ was estimated by combining the N–N distance (3.79 \AA) observed in the crystal structure of $[3][BF_4]_2$ (see above) with twice the Fe–N distance observed in the crystal structure of **1** (5.60 \AA)^{S8} to give a total length of 14.99 \AA .

Cyclic Voltammetry

Electrochemical investigations in dichloromethane showed that the redox behavior of both compounds $[4][BF_4]_2$ and $[5][BF_4]_2$ was broadly similar (Table S3). The experiments using NBu_4PF_6 as the electrolyte display two diffusion controlled one-electron reversible oxidations along with a third quasi-reversible one-electron oxidation. Given the proximity of the first two oxidation events to one another, determination of the peak currents was not feasible. However, the values of $E_{1/2}$ remained constant with varying scan rate for the first two oxidation events in both compounds indicating reversible behavior. Table 1 and Figure S7 show that the oxidation events observed for $[5][BF_4]_2$ occur at a potential approximately 100 mV greater than those seen for $[4][BF_4]_2$ in both electrolytes. When $NBu_4[B\{C_6H_3(CF_3)_2-3,5\}_4]$ was used as the electrolyte only two diffusion controlled one-electron oxidation events were observed, the third occurring above the decomposition potential of the

solvent, the peak separation was increased by the alteration of the electrolyte suggesting that the oxidation events are metal centered rather than ligand centered, this is consistent with the expected redox properties of iron compounds. Electrochemical investigations of **[4]**[BF₄]₂ in acetonitrile showed broadly similar behavior to that observed in dichloromethane (Figure S8), though the complex was unstable and decomposed slightly over the course of the experiment. Complex **[5]**[BF₄]₂ decomposed in acetonitrile under electrochemical conditions in a matter of minutes and as such no useful data could be obtained.

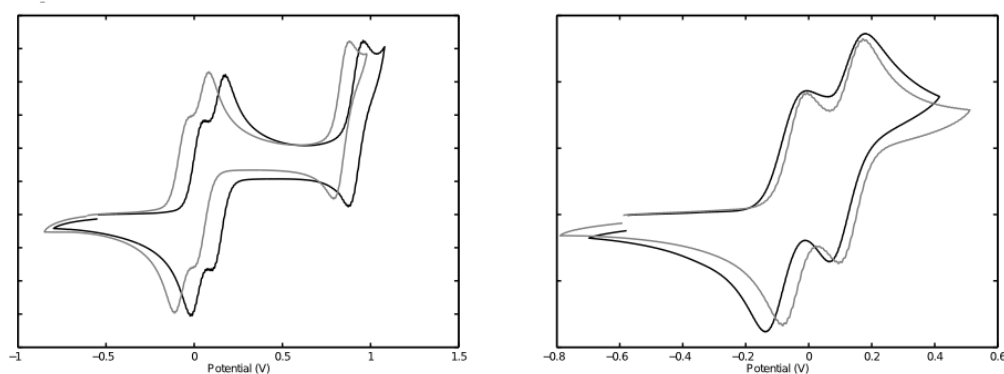


Figure S7. Cyclic voltammograms obtained for **[4]**[BF₄]₂ (black) and **[5]**[BF₄]₂ (grey) in dichloromethane using 0.1 M NBu₄PF₆ (left) or NBu₄[C₆H₃(CF₃)₂]₄ (right) as the electrolyte relative to the FeCp₂/FeCp₂⁺ couple at 0.00 V.

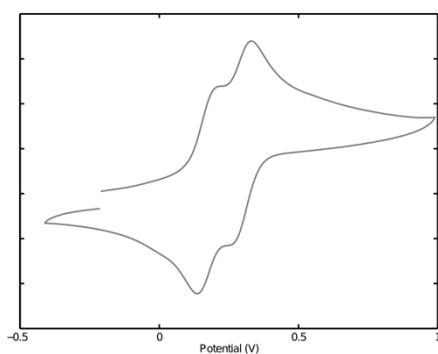


Figure S8. Cyclic voltammogram obtained for **[4]**[BF₄]₂ in acetonitrile using 0.1 M NBu₄PF₆ as the electrolyte relative to the FeCp₂/FeCp₂⁺ couple at 0.00 V.

	CH ₂ Cl ₂ /NBu ₄ PF ₆		CH ₂ Cl ₂ /NBu ₄ BAR ₄ ^F		MeCN/ NBu ₄ PF ₆
	4	5	4	5	4
<i>E</i> _{1/2} (1)	0.02	-0.05	-0.04	-0.07	0.14
<i>E</i> _{1/2} (2)	0.15	0.07	0.14	0.13	0.26
<i>E</i> _{1/2} (3)	0.92	0.83	—	—	—

Table S3. Electrochemical data for trimetallic iron cyanoacetylides relative to the FeCp₂/[FeCp₂]⁺ couple at 0.00 V.[†]

References

- S1. M. I. Bruce, K. Costuas, B. G. Ellis, J.-F. Halet, P. J. Low, B. Moubaraki, K. S. Murray, N. Ouddaï, G. J. Perkins, B. W. Skelton, and A. H. White, *Organometallics*, 2007, **26**, 3735–3745.
- S2. E. M. Long, N. J. Brown, W. Y. Man, M. A. Fox, D. S. Yufit, J. A. K. Howard, and P. J. Low, *Inorganica Chimica Acta*, 2012, **380**, 358–371.
- S3. R. B. Bedford, E. Carter, P. M. Cogswell, N. J. Gower, M. F. Haddow, J. N. Harvey, D. M. Murphy, E. C. Neeve, and J. Nunn, *Angew. Chem. Int. Ed.*, 2012, **52**, 1285–1288.
- S4. G. R. Fulmer, A. J. M. Miller, N. H. Sherden, H. E. Gottlieb, A. Nudelman, B. M. Stoltz, J. E. Bercaw, and K. I. Goldberg, *Organometallics*, 2010, **29**, 2176–2179.
- S5. M. Krejčík, M. Daněk, and F. J. Hartl, *J. Electroanal. Chem.*, 1991, **317**, 179–187.
- S6. O. V. Dolomanov, L. J. Bourhis, R. J. Gildea, J. A. K. Howard and H. Puschmann, *J. Appl. Cryst.*, 2009, **42**, 339–341.
- S7. G.M. Sheldrick, *Acta Cryst.*, 2008, **A64**, 112–122
- S8. M. E. Smith, R. L. Cordiner, D. Albesa-Jové, D. S. Yufit, F. Hartl, J. A. Howard, and P. J. Low, *Can. J. Chem.*, 2006, **84**, 154–163.